The team used **QUOKKA** to search for such features when a magnetic field was applied in the material's plane. Importantly, they found no evidence of static magnetic textures, such as skyrmions or other chiral structures.[2] This absence was as significant as a positive detection because it ruled out conventional explanations[4] and strengthened the case that the observed AHE originates from dynamic, rather than static, magnetic behavior.

QUOKKA's ability to reveal what was not there helped clarify what was. By ruling out field-induced static chirality, the SANS measurements supported the team's theory: the AHE arises solely from fluctuating spins interacting with conduction electrons, with ytterbium ions subtly influencing spin orientation and enhancing fluctuations at low temperatures.

In summary, this research demonstrates how complex magnetic materials can exhibit unexpected quantum behaviors that may be useful for future technology. The work led by Dai shows that even materials with simple collinear antiferromagnetic structures can display rich electronic responses when their spins fluctuate appropriately. Neutron scattering, particularly using instruments like **QUOKKA**, was crucial in uncovering the hidden dynamics behind these effects. As scientists seek efficient, low-energy methods to manipulate electron spin, discoveries like this expand the possibilities and open new directions for quantum materials research. (Reported by Chun-Ming Wu)

This report features the work of Pengcheng Dai and his collaborators published in Phys. Rev. Lett. ***134****, 186501(2025).*

ANSTO QUOKKA – Small-angle Neutron Scattering

- SANS
- Condensed-matter Physics

References

1. N. Nagaosa, J. Sinova, S. Onoda, A. H. MacDonald, N. P. Ong, Rev. Mod. Phys. **82**, 1539 (2010).
2. W. Yao, S. Liu, H. Kikuchi, H. Ishikawa, Ø. S. Fjellvåg, D. W. Tam, F. Ye, D. L. Abernathy, G. D. A. Wood, D. Adroja, C.-M. Wu, C.-L. Huang, B. Gao, Y. Xie, Y. Gao, K. Rao, E. Morosan, K. Kindo, T. Masuda, K. Hashimoto, T. Shibauchi, P. Dai, Phys. Rev. Lett. **134**, 186501 (2025).
3. W. Wang, M. W. Daniels, Z. Liao, Y. Zhao, J. Wang, G. Koster, G. Rijnders, C.-Z. Chang, D. Xiao, W. Wu, Nat. Mater. **18**, 1054 (2019).
4. S. Nakatsuji, N. Kiyohara, T. Higo, Nature **527**, 212 (2015).

Ordered Spin Structures of Multiferroic and Skyrmion Compounds

Neutron scattering is a unique probe for spin correlations.

The neutron diffraction technique, developed in the 1930s, has become an indispensable tool for investigating complex behaviors in magnetic, multiferroic, and strongly correlated materials. Due to the neutron's intrinsic spin and charge neutrality, it interacts directly with magnetic moments, enabling precise determination of magnetic ordering, spin textures, and subtle structural distortions that often accompany electronic phase transitions. In multiferroics, where electric and magnetic orders coexist and frequently couple in intricate ways, neutron diffraction reveals the symmetry-breaking mechanisms that link lattice, charge, and spin degrees of freedom. In strongly correlated systems, neutron scattering uncovers collective excitations, long-range correlations, and hidden order parameters that conventional probes cannot detect. By providing sensitivity to both nuclear and magnetic structures, neutron diffraction offers a coherent, microscopic view of how competing interactions shape exotic ground states and emergent phenomena, making it a cornerstone technique in contemporary condensed matter physics.

For researchers in Taiwan, the Australian Centre for Neutron Scattering (ACNS) at Australian Nuclear Science and Technology Organisation (ANSTO) offers a unique opportunity. The Neutron Group of the NSRRC, based at ACNS, can assist Taiwan researchers in various ways. Hung-Duen Yang (National Sun Yat-sen University)

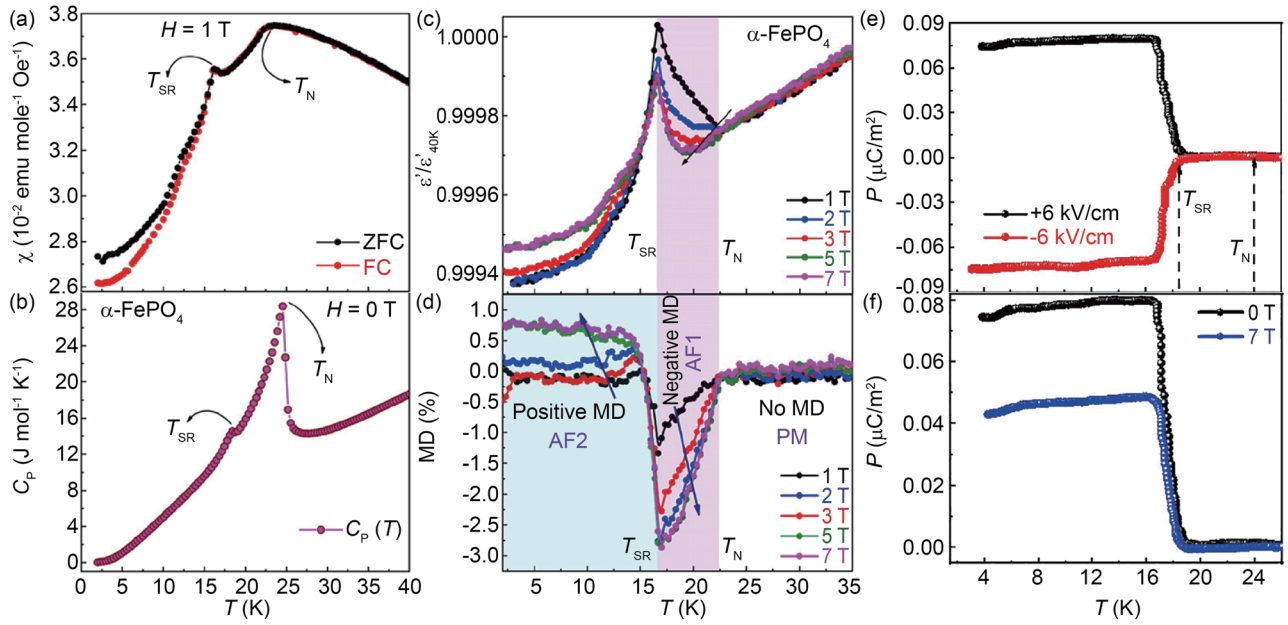

Fig. 1: (a) χ vs. T at H = 1 T (Zero field cool/Field cool) for α-$FePO_4$ showing the presence of two distinct magnetic transitions at T ≈ 25 K and T_{SR} ~ 17 K, which are further supported by (b) specific heat measurements at H = 0 T. (c) ε' vs. T curves under various H. (d) MD%, calculated from ε' vs. T, indicates a sign change in MD from negative to positive at the onset of T_{SR}. (e) Electric polarization (P), measured after cooling under different poling fields, is determined by integrating current (I) over time at H = 0 T. (f) Electric polarization under different H demonstrates that the magnetic field suppresses polarization. [Reproduced from Ref. 1]

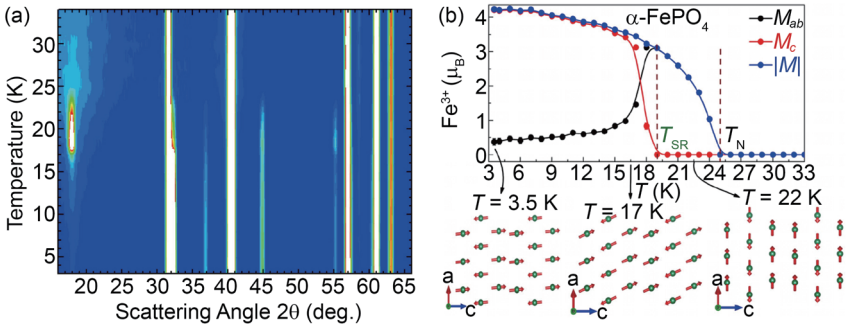

Fig. 2: (a) Temperature-dependent NPD patterns of α-$FePO_4$. The long-range magnetic ordering at T_N = 25 K and a redistribution of magnetic diffraction intensities at T_{SR} = 17 K. (b) The refined magnetic moment as a function of the temperature illustrates the evolution of the easy axis from the ab-plane to the c-axis. Spin structures are shown at three selected temperatures. [Reproduced from Ref. 1]

is a long-term user of ACNS and has achieved notable results in recent years. Two recent works by Yang and collaborators are highlighted in this report. The α-Iron phosphate (α-$FePO_4$), known as berlinite, crystallizes into a non-centrosymmetric trigonal $P3_121$ structure. In the compound, the magnetic Fe^{3+} ions form a two-dimensional layered triangular lattice on the ab-plane. Magnetic susceptibility and specific heat reveal two magnetic transitions at ~25 K and ~ 17 K, as shown in **Figs. 1(a) and 1(b)**. The reduction of magnetization below ~ 25 K indicates an antiferromagnetic order, and the second anomaly is associated with the spin reorientation transition (SR), as confirmed by the neutron diffraction experiment. The temperature dependence of dielectric constant (ε') and magnetodielectric response (MD) is shown in **Figs. 1(c) and 1(d)**. A clear correlation between the magnetic and electrical degrees of freedom is exhibited. The value of the dielectric constant is suppressed and enhanced in the temperature ranges ~17 K < T < ~25 K and T < ~17 K, respectively, manifesting the negative and positive MD effects. **Figures 1(e) and 1(f)** show the electric polarization measured in the compound. The sign of the P is flipped while reversing the polling electric field direction. The application of H significantly suppresses the electric polarization P, suggesting that P may be linked to the magnetic structure that responds to the applied magnetic field. Noticeably, the electrical polarization P exists only below ~17 K, suggesting that α-$FePO_4$ might be a Type-II multiferroic material, of which P is connected to the low-temperature magnetic phase.

The neutron powder diffraction (NPD) experiments were conducted on the high-intensity powder diffractometer **WOMBAT** at the Open Pool Australian Lightwater reactor (OPAL) at ANSTO. The temperature-dependent diffraction patterns are shown as a color contour in **Fig. 2(a)**. Upon cooling, new diffraction peaks of magnetic origin appear below ~24 K, and these peaks can be indexed with the magnetic wave vector k = (0, 0, 1/2), indicating that the magnetic unit cell is twice the size of the crystal structure unit cell. With further cooling, the magnetic (0, 0, -3/2) peak at 2θ ~18° reverses its trend at ~17 K, while the other peaks increase. Analysis of the NPD

patterns reveals that the spin structure is collinear antiferromagnetic over the entire temperature range studied. The spins in the triangular layer are parallel, and the ferromagnetic layers are stacked alternately along the *c*-axis. The refined magnetic moment as a function of the temperature is shown in **Fig. 2(b)**. Initially, the spins lie in the ab-plane and tilt upward below ~17 K, suggesting a spin-rotation transition. Based on previous neutron studies and the present NPD analysis, the spin structure remains essentially unchanged through the transition, and α-$FePO_4$ is not a conventional Type-II multiferroic. This observation encourages further studies using Raman spectroscopy and density functional theory (DFT) calculations, leading to the conclusion that the spin-dependent p-d hybridization mechanism potentially explains the observed polarization.

Another case is the study of the polar compound $VOSe_2O_5$ ($P4_{CC}$).[2] This compound is a rare example of a bulk material that hosts Néel-type skyrmions. In this work, AC magnetic susceptibility measurements were performed at various temperatures, magnetic fields, and pressures, resulting in a detailed phase diagram. In the low-field regime, two magnetic transitions, labeled T_{C1} (~7.4 K) and T_{C2} (~4.0 K), are identified. The phase between T_{C2} and T_{C1} is sensitive to the magnetic field: successive phase transitions occur as the magnetic field is increased. Furthermore, a small region just below the order-disorder boundary is marked as the "A" phase in **Figs. 1(a) and 1(b)**. Remarkably, hydrostatic pressure can stabilize the skyrmion phase. The area of the skyrmion phase in the H-T phase diagram increases by approximately three times under a pressure of 14.21 kbar, as shown in **Fig. 3(b)**. Neutron diffraction is useful for characterizing these phases.

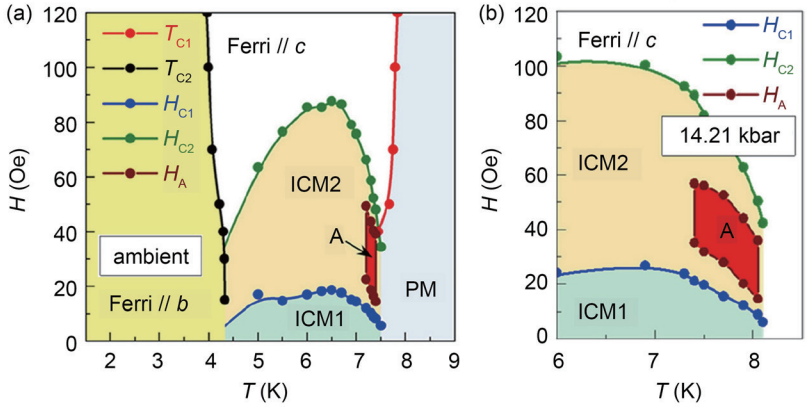

Fig. 3: *H-T* phase diagrams of $VOSe_2O_5$ (a) at ambient pressure and (b) under pressure P = 14.21 kbar. Both diagrams show the critical fields H_{C1} and H_{C2}, which indicate transitions between magnetic phases: ferrimagnetic (Ferri//*c*), ICM1, and ICM2. The A zone represents the skyrmion phase, and in (b), this phase expands by approximately threefold under 14.21 kbar, demonstrating that pressure effectively influences skyrmion phase stability. [Reproduced from Ref. 2]

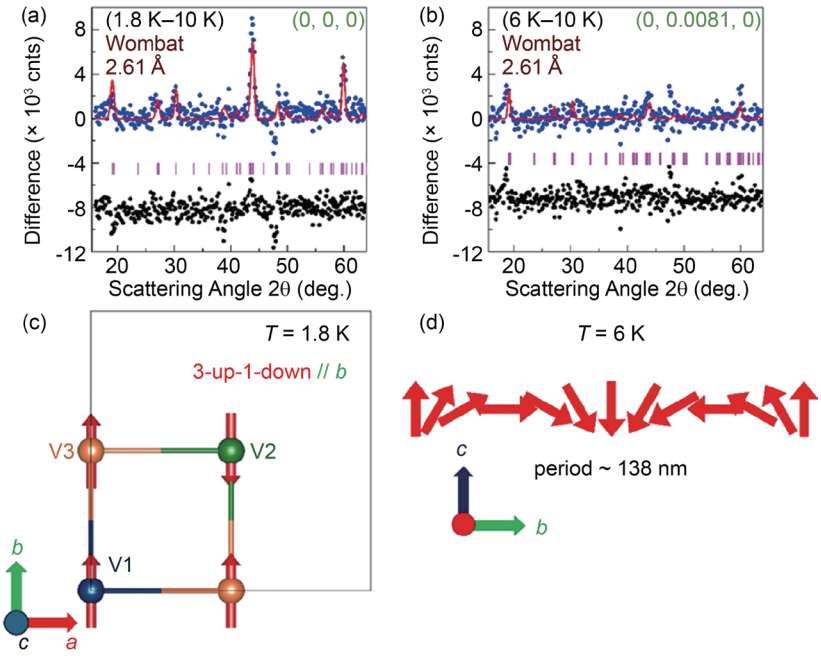

Fig. 4: (a) Neutron diffraction difference patterns between 1.8 K and 10 K highlight the pure magnetic contribution and corresponding refinement. (b) Difference patterns between 6 K and 10 K, with magnetic refinement. Purple ticks indicate magnetic reflections. The distinct temperature-dependent patterns reveal two different magnetic structures. (c,d) Illustrations of the magnetic structures at T = 1.8 K and 6 K, respectively. At 1.8 K, a three-up-one-down collinear ferrimagnetic configuration is aligned along the *b*-axis. At 6 K, an incommensurate cycloidal structure emerges, with spins rotating within the *bc*-plane and a modulation period of approximately 138 nm. This temperature-dependent evolution of the magnetic structure highlights the inherent magnetic anisotropies in this system. [Reproduced from Ref. 2]

The NPD experiments are conducted on the high-intensity powder diffractometer, **WOMBAT**. Magnetic structure determination for low-spin magnets, which may be influenced by quantum fluctuations, is generally challenging due to extremely weak magnetic signals in NPD patterns. In earlier NPD studies using a high-resolution powder diffractometer, the weak magnetic signal was not detected; however, analyzable data were obtained with the high-intensity diffractometer. **Figures 4(a) and 4(b)** present the analysis of magnetic diffraction patterns, obtained by subtracting the 10 K pattern (above T) from those collected in the ordered state. Although the data quality is not optimal, it is sufficient for comparing symmetry-constrained models.

A collinear ferrimagnetic model with spins aligned along the *b*-axis is supported by the magnetic diffraction pattern at 1.8 K. The four V^{4+} spins in the unit cell are arranged in a three-up, one-down configuration, as shown in **Fig. 4(c)**, consistent with earlier DFT results.[3] The spin structure between T_{C1} and T_{C2} that hosts a skyrmion phase is expected to be incommensurate, as indicated by various chiral compounds that exhibit skyrmion lattice phases. A recent small-angle neutron scattering (SANS) experiment reveals a magnetic propagation vector k = (0, 0.0081, 0) from a single crystal sample.[4] For such an extremely long period-modulated spin structure, the period or magnetic structure cannot be determined solely by conventional NPD. By combining the propagation vector obtained from the SANS experiment with the magnetic diffraction pattern, one can distinguish among candidate models and conclude that a cycloidal spin structure, with spins evolving in the bc-plane as illustrated in **Fig. 4(d)**, is present.

In this report, two applications of NPD in condensed matter research are summarized, demonstrating that neutron diffraction provides unique information not accessible through other experimental techniques. (Reported by Chin-Wei Wang)

This report features the works of Hung-Duen Yang and his collaborators published in Phys. Rev. B ***111****, 214418 (2025), and Phys. Rev. B* ***112****, 024441 (2025).*

ANSTO WOMBAT – High-Intensity Powder Diffractometer

- NPD
- Materials Science, Chemistry, Condensed-matter Physics

References

1. D. C. Kakarla, A. Tiwari, Y. H. Tseng, T. W. Yen, H. C. Wu, C. W. Wang, M.-J. Hsieh, J.-Y. Lin, A. Pal, C. Dhanasekhar, D. P. Gulo, H. L. Liu, H. D. Yang, Phys. Rev. B **111**, 214418 (2025).
2. T. W. Kuo, C. C. Chen, D. C. Kakarla, A. Tiwari, C. W. Wang, M. Gooch, L. Z. Deng, C. W. Chu, H. D. Yang, H. C. Wu, Phys. Rev. B **112**, 024441 (2025).
3. S.-H. Kim, P. S. Halasyamani, B. C. Mottot, R. Sechadri, M. A. Green, A. S. Sefat, D. Mandrus, Chem. Mater. **22**, 5074 (2010).
4. T. Kurumaji, T. Nakajima, V. Ukleev, A. Feoktystov, T. Arima, K. Kakurai, Yoshinori Tokura, Phys. Rev. Lett. **119**, 237201 (2017).

Neutron Reflectometry Probes Critical Interface Effects in Ferroelectric $Hf_{0.5}Zr_{0.5}O_2$ Films

The interfacial structure of ferroelectric $Hf_{0.5}Zr_{0.5}O_2$ thin films has been shown to strongly influence device performance.

Introducing Zr into HfO_2 thin films lowers the crystallization temperature for the ferroelectric orthorhombic phase and promotes robust ferroelectric properties. A team led by Miin-Jang Chen (National Taiwan University) and Tzu-Yen Huang (NSRRC) systematically investigated the depth-dependent structure of ferroelectric $Hf_{0.5}Zr_{0.5}O_2$ (HZO) thin films. HZO metal–ferroelectric–metal (MFM) devices with W electrodes were fabricated by atomic layer deposition using thermal (THE), plasma-assisted (PLA), and atomic layer annealing (ALA) processes, and their ferroelectric properties were evaluated.

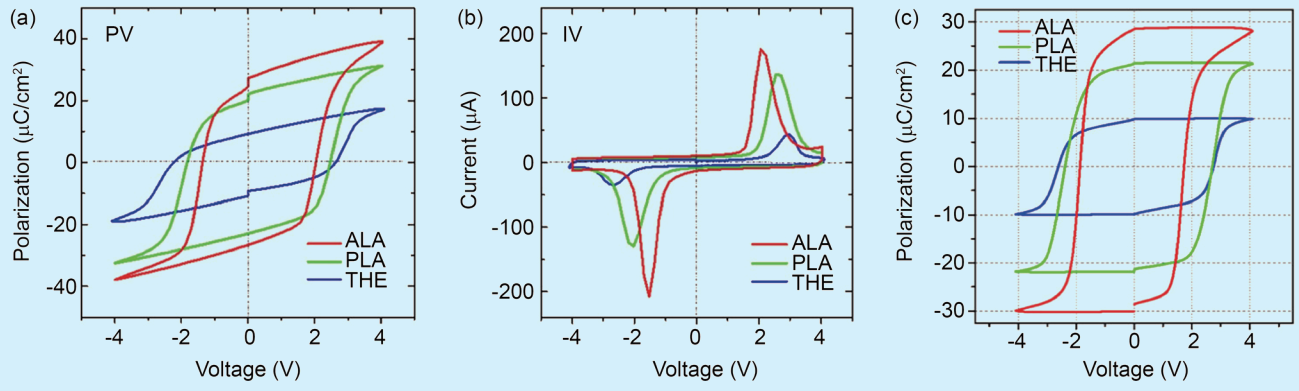

Fig. 1: (a) P–V hysteresis and (b) I–V switching responses show that the ALA device exhibits the largest Pr and the strongest switching current. (c) PUND-derived switching polarization measured with a 4 V pulse amplitude at 2 kHz confirms the most pronounced ferroelectric switching for the ALA-treated HZO film. [Reproduced from Ref. 1]